# Enhanced Mineralization of the Tibial Epiphyseal Plate in the Rat Following Propylthiouracil Treatment: A Histochemical, Light, and Electron Microscopic Study [1]

LYLE C. DEARDEN
*Department of Anatomy, University of California, Irvine, California College of Medicine, Irvine, California 92664*

*ABSTRACT* Following treatment with propylthiouracil, most chondrocytes in the reserve and upper proliferation zones in the tibial epiphyseal plate exhibit degenerate ultrastructural morphology. In the extracellular matrix, sulfated mucopolysaccharide is reduced, matrix vesicles are increased both in number and in size, apatite crystals are present in all zones, and mineralization is enhanced.

In post-treatment recovery, chondrocyte degeneration decreases; however, the extracellular matrix is considerably delayed in returning to conditions comparable to those in corresponding controls and this is indicated by the continued presence of apatite crystals in abnormal locations.

Chondrocyte degeneration, sulfated mucopolysaccharide, and matrix vesicles, are discussed as they relate to the mineralization process.

Two consistent themes repeatedly occur in the literature relative to cartilage mineralization: (1) in the zone of calcification there is a decrease in sulfated mucopolysaccharide (Schubert and Pras, '68; Campo, '70; Smith, '70) and, (2) matrix vesicles, probably of cellular origin, seem to be the sites of initial calcification, i.e., the deposition of calcium phosphate which subsequently is converted to hydroxyapatite crystals (Bonucci, '67, '69, '70, '71; Anderson, '68, '69; Anderson, Matsuzawa, Sajdera and Ali, '70; Ali, Sajdera and Anderson, '70; Matsuzawa and Anderson, '70; Alcock, '72; Thyberg and Friberg, '70, '72; Thyberg, '72).

The relationship of a decrease in sulfated mucopolysaccharide to the calcification process has received different interpretations. On the one hand, it is claimed that calcification is dependent upon a failure to maintain the appropriate level of this polysaccharide in the intercellular matrix (Hass, '43), while, on the other hand it is postulated that the turnover of sulfated mucopolysaccharide is not closely related to the calcification process (Weatherell, Bailey and Weidmann, '64). Regardless of these and other divergent opinions (Miller, Waldman and McLean, '52; Glimcher, '60; Dulce, '60; Sobel, '60), it appears to be well established that a decrease in sulfated mucopolysaccharide occurs in the calcification zone under normal conditions.

The concept that matrix vesicles constitute the initial locus of cartilage calcification seems less controversial. Recent ultrastructural evidence from a variety of calcifying tissues (cartilage, bone, teeth) (Ali et al., '70; Anderson et al., '70; Anderson and Sajdera, '71; Alcock, '72; Thyberg, '72; Bernard, '72; Eisenman and Glick, '72) is supportive.

In a recent experimental study of long-term recovery of the tibial epiphyseal plate in immature Long-Evans rats following treatment with 6-propylthiouracil (PTU), a marked increase in the number of matrix vesicles was noted in conjunction with a reduction of sulfated mucopolysaccharide in the extracellular matrix. In view of the foregoing, this suggested that treatment

Received Mar. 26, '73. Accepted July 26, '73.

[1] Supported in part by the Easter Seal Research Foundation.

with PTU might enhance mineralization. Therefore, the present paper presents the effects of PTU-treatment on chondrocytes and relates these to the mineralization process with particular reference to sulfated mucopolysaccharides and matrix vesicles.

## MATERIALS AND METHODS

Forty male Long-Evans rats, forty-two days old and weighing approximately 121 gm were used in this study. They were maintained individually in 7 by 7 by 10 inch wire mesh floored cages at a temperature of 21.2–26.7°C. The light-dark cycle was set at 14–10 hours. The standard diet was finely powdered Purina Laboratory Chow. Water was available *ad lib.*

Growth retardation was produced by adding 6-propylthiouracil (USP-synthetic-Mann Research Laboratories) to the standard powdered diet to make a concentration of 0.1%. This diet was continued for 18 days at which time the difference between the mean body weight of experimentals and the mean body weight of controls approximately equaled the weight difference between controls and animals fasted for two days. Rats were divided into four groups, each with four controls and six experimental animals. Control rats received the standard powdered diet without PTU. Experimental animals and corresponding controls were sacrificed at 0, 5, 12 and 26 days after discontinuation of PTU-treatment. All animals survived to the end of the experiment.

At autopsy, tibial heads and the proximal diaphyseal shaft from both legs were removed and one was placed in 4% glutaraldehyde in Millonig's phosphate buffer (Millonig, '61) for electron microscopy, while the other was fixed in either neutral 10% formalin or Bouin's solution for light microscopy.

*For electron microscopy,* tissues were stripped of flesh and 1 mm thick coronal slices across the width of each tibial head were sequentially cut with a razor blade. Glutaraldehyde fixation continued for two hours. Tissues were post-fixed for one hour in 1% $OsO_4$, dehydrated in a graded series of acetone and embedded in Epon 812. Before the final Epon change, tissue slices were cut sequentially into blocks (approximately 1 × 2 × 3 mm) and each block was properly oriented in Epon filled capsules. Thick sections (0.5–1.0 $\mu$) were cut with a Reichert ultramicrotome and stained with 0.5% aqueous toluidine blue. Areas for thin sectioning were selected; thin sections (grey to gold) were cut, mounted on Formvar-coated copper grids, observed after staining with uranyl acetate and lead citrate (Reynolds, '63), and photographed with a Philips EM 300 electron microscope.

Acid mucopolysaccharides were identified electron microscopically by means of Mowry's modification of colloidal iron (Curran, Clark and Lovell, '65; Matukas, Panner and Orbison, '67). Sulfated mucopolysaccharides were identified by staining with bismuth nitrate (Smith, '70). As an aid in identification of the structures stained, alternate thin sections were stained with uranyl acetate and lead citrate.

Other specimens were fixed in 4% formalin and digested at 37°C for 12 hours with hyaluronidase following the technique of Bonucci ('70). Controls, in buffers, without hyaluronidase were incubated for the same period of time and at the same temperature. Control and experimental specimens were dehydrated with acetone, embedded in Epon, sectioned, and stained with either bismuth nitrate, or Mowry's colloidal iron.

*For light microscopy,* following standard dehydration and paraffin embedding, 7–8 $\mu$ sections were cut and tissues were stained with hematoxylin and eosin; periodic acid-Schiff (PAS) for neutral polysaccharides (glycogen and neutral mucopolysaccharides — magenta); Mowry's alcian blue (pH 2.5) for acid mucopolysaccharides (blue); Mowry's modification of Müller's colloidal iron method (pH 1.3) for sulfated mucopolysaccharides (blue) (Mowry, '58; Foldes, Modis and Suveges, '65). Some of these latter sections were counter stained with PAS. Other sections were stained with Gomori's aldehyde fuchsin which is claimed to be specific for sulfated polysaccharides (Spicer, '62).

For comparison with paraffin sections, some thick plastic sections were deplasticized and stained with PAS, Mowry's alcian blue (pH 2.5) or with Mowry's colloidal iron (pH 1.3). Others were deplasticized

and stained with the Pearson silver-gelatin technique for calcium salt deposition (Rosenquist, Slavin and Bernick, '71).

## OBSERVATIONS

*Histochemistry: Optical microscopy.* (The different zones in chondrocyte maturation are indicated in figure one). The extracellular matrix in controls and in all experimental rats contained sulfated mucopolysaccharide (blue with alcian blue, blue with colloidal iron, purple with aldehyde fuchsin). In controls, sulfated mucopolysaccharide in the extracellular matrix was most prominent in the proliferation zone and decreased toward the zone of chondrolysis. Although there was some variation, sulfated mucopolysaccharide was always more pronounced and more extensive in the matrix of controls than it was in experimental rats at the end of the treatment period (compare figs. 1A,B). Although sulfated mucopolysaccharide increased in PTU-treated rats in later recovery periods, in the terminal recovery period it did not correspond with that noted in controls.

Glycogen deposition (PAS-positive) was much more prominent in cells in all zones than in cells in corresponding zones in controls (compare figs. 2A,B). Matrix vesicles (PAS-positive; metachromatic with toluidine blue; negative with alcian blue, colloidal iron or aldehyde fuchsin) were larger and more numerous, particularly in the proliferation zone, than they were in controls. Glycogen deposition was subsequently reduced and matrix vesicles became smaller and less numerous; however, return to conditions comparable to those in controls was considerable delayed.

Calcium deposition was enhanced following treatment with PTU (compare figs. 3A,B, insets) and continued to be more extensive in all recovery periods than in corresponding controls.

*Histochemistry: Electron microscopy.* Following colloidal iron or bismuth nitrate staining of formalin or glutaraldehyde fixed thin sections, the outer surface of cytoplasmic dense bodies, the cell membrane, granules on the membrane, lacunar granules, part of the contents of Golgi vacuoles, and matrix granules (probably from Golgi vacuoles) were positive with both stains in controls and in PTU-treated rats (fig. 4A). The outer surface of matrix vesicles was positive with either stain in controls and in PTU-treated rats in glutaraldehyde fixed tissue (fig. 4B), but negative in formalin fixed tissue; collagen was negative with both stains regardless of the fixative used (fig. 4B). The extracellular matrix was more positive with either stain in controls than it was in the PTU-treated rats.

After hyaluronidase digestion and staining with either bismuth nitrate or colloidal iron, the outer surface of cytoplasmic dense bodies, the cell membrane, granules on the membrane, lacunar granules, the content of Golgi vacuoles, matrix granules, and the outer surface of matrix vesicles were all negative (fig. 4C).

*Electron microscopy.* At the end of the treatment period chondrocyte degeneration was extensive and two aspects of degeneration were demonstrable. Chondrocytes with an abnormal cytoplasm and a pyknotic nucleus were common; they frequently occurred in long columns (fig. 5). Golgi vacuoles were prominent in these cells but not in other degenerate cells. Less degenerate cells, particularly in the reserve and upper proliferation zones, exhibited ultrastructural abnormalities (fig. 6A) when compared with corresponding cells in controls (fig. 6B). Nuclei were dense, frequently indented, and their chromatin pattern was abnormal; cytoplasmic vacuolization was frequently noted; glycogen deposition was enhanced; lipid was noted in the cytoplasm frequently in conjunction with glycogen; mitochondria were swollen and vacuolated; the Golgi complex was not prominent; the endoplasmic reticulum (ER) was reduced; cytoplasmic dense bodies (presumably lysosomes) were common and were more frequently noted than in controls (fig. 6C). All of the criteria used to designate degeneration corresponded with those noted in chondrocytes by previous investigators (Silberberg, Silberberg and Feir, '64, '66). Additionally, fibrillar microscars (fig. 7) developed during or after cell disintegration (Silberberg and Hasler, '66) were commonly noted. Collagen fibrils composing these microscars were regularly banded and were much thicker (600–

1200 Å vs 200 Å) than adjacent fibrils (inset, fig. 7).

With the exception of enhanced glycogen deposition, the ultrastructure of chondrocytes in the lower proliferation and hypertrophic zones was comparable to that of corresponding controls.

Matrix vesicles in all zones were generally larger (4,000 vs 2,000 Å), more numerous and frequently more electron dense than in the matrix of controls (compare insets (figs. 6A,B). They seemed to be derived, at least in part, from disintegrating chondrocytes (figs. 8A,B) and, with the exception of the reserve zone, they were most commonly found in longitudinal septa. More infrequently they were found in pericellular lacunae and in transverse septa. As previously indicated, their outer surface was positive after staining with bismuth nitrate or colloidal iron. In chondrocytes in all zones some cytoplasmic dense bodies corresponded in size and in configuration with matrix vesicles and were also positive with these same stains.

Apatite crystals were present in all zones in the PTU-treated rats (see inset, fig. 5). They were not present in the proliferation zone in controls and they were less numerous in the other zones than they were in the experimental rats (compare figs. 9A,B, for example). They occurred most often as needle-shaped crystals in association with matrix vesicles but not necessarily in contact with vesicles. In some instances they seemed attached to the outer lamina of the trilaminar membrane of vesicles.

The presence of numerous matrix vesicles and apatite crystals, particularly in the proliferation zone, seemed to corroborate the light microscope findings relative to enhanced calicification.

In subsequent recovery periods chondrocyte recovery was indicated by an increase in the amount of ER, a decrease in cytoplasmic vacuolization, and the Golgi complex corresponded with that noted in controls. Mitochondrial swelling and vacuolization decreased; however, mitochondria were slower than other organelles in demonstrating recovery. Matrix vesicles decreased both in number and in size. However, there was still some degenerate ultrastructure in some cells, persistent columns, of degenerate chondrocytes (fig. 10), and continued abnormal occurrence of apatite crystals in the proliferation zone (see inset, fig. 10).

## DISCUSSION

Following treatment with PTU chondrocyte degeneration is increased. There is a marked reduction of sulfated mucopolysaccharide in the extracellular matrix and this is in keeping with a similar reduction in skin after treatment with PTU (Schiller, Glover and Dorfman, '62). The greatest preponderance of sulfated mucopolysaccharide is in the lower reserve and upper proliferation zone in controls while, in PTU-treated rats, in these same areas, it is markedly reduced. The ultrastructure of most chondrocytes in these same areas in the experimental rats is indicative of degeneration and this suggests altered chondrocyte metabolism. The amount of ER is reduced and this implies a reduction in protein synthesis which agrees with previous findings regarding inhibition of protein synthesis following treatment with PTU (Dearden and Mosier, '71) and with cortisone (Dearden and Mosier, '72). Since secretory protein from the ER is thought to be transported by means of small vesicles to Golgi vacuoles (Caro and Palade, '64; Jamieson and Palade, '67; Holtrop, '72) where sulfation occurs, (Godman and Lane, '64; Neutra and Leblond, '66; Rohr and Walter, '66; Rambourg, Hernandez and Leblond, '69) and the sulfated protein polysaccharide complex is subsequently extruded into the matrix (Holtrop, '72), a decrease in protein synthesis might relate to a reduction of sulfated mucopolysaccharide. Additionally, this reduction would also be consistent with a decrease in the Golgi complex and with an increase in the number of degenerate and/or cells judged to be destined for disintegration and death (fig. 5). Normally, sulfated mucopolysaccharide decreases in the early calcification stages (Schubert and Pras, '68; Campo, '70; Smith, '70) and the presence of apatite crystals in the proliferation zone in the experimental rats suggests premature mineralization. At first glance it would appear that mineralization is closely related to the observed decrease in sulfated mucopoly-

saccharide. However, in subsequent recovery periods, while synthesis of sulfated mucopolysaccharide is increasing and its distribution is extending toward the zone of calcification, apatite crystals are still present in the proliferation zone. Thus a close relationship is not necessarily indicated and this corresponds with previous findings (Weatherell et al., '64).

The accumulation of intracellular glycogen can be related to chondrocyte degeneration and senescence (Silberberg et al., '64), as well as to a failure of incorporation in the glycolytic pathway (Weatherell et al., '64). These findings, related to the present study would imply, in the first case, altered chondrocyte function, possibly leading to an increase in cell death, and, in the second, an inhibition of synthesis of sulfated mucopolysaccharide.

Concurrent with the reduction of sulfated mucopolysaccharide, matrix vesicles increase both in number and in size. This might not seem to be consistent with an increase in the number of degenerate cells. However, matrix vesicles have been proposed to originate from degenerating cells (Bonucci, '67, '70; Anderson, '68, '69) or from lysosomes (Thyberg and Friberg, '70, '72; Thyberg, '72). In this study, there is morphological evidence of their origin from degenerating cells (figs. 8A,B). Histochemically, matrix vesicles and cytoplasmic dense bodies (presumably lysosomes) are positive after staining with bismuth nitrate or colloidal iron (fig. 4A), and their close proximity (lacunar space and just under the cell membrane) suggests that some matrix vesicles may be extruded lysosomes. Therefore, in view of the numerous degenerate chondrocytes and of the increased number of lysosomes, an increase in matrix vesicles would not be unexpected. Since matrix vesicles have been proposed as the initial sites of cartilage calcification (Bonucci, '71; Alcock, '72) the increase in number and size of matrix vesicles in the present study suggests premature calcification. The enhanced calcium deposition at the end of the treatment period is supportive of this suggestion. Deposition of apatite crystals is increased in all zones and their association with matrix vesicles, which are particularly numerous in the proliferation zone, indicates that mineralization is also occurring prematurely.

In subsequent recovery periods there is a decrease in the number of degenerate chondrocytes, a decrease in the number and size of matrix vesicles, an increase in production of sulfated mucopolysaccharide, and glycogen deposition corresponds with that noted in controls. These findings suggest recovery from the effects of treatment. However, apatite crystals persist in all zones and in all recovery periods. While conditions favoring enhanced mineralization are present at the end of the treatment period, they do not prevail in the terminal recovery period. The continued presence of apatite crystals in abnormal locations under conditions which would seem to favor the initiation of mineralization in the hypertrophic zone, indicates the need for additional study.

In summary, following treatment with PTU, mineralization of the tibial epiphyseal plate is increased, and this seems related to chondrocyte degeneration and/or to altered chondrocyte metabolism. Whether the presence of apatite crystals and premature mineralization of the proliferation zone in the terminal recovery period is directly or indirectly related to PTU treatment, remains obscure.

ACKNOWLEDGMENTS

The author wishes to express his gratitude to Teresa Espinosa, Lynn Wiley, and Paula Davis, for their expert and skillful technical assistance.

LITERATURE CITED

Alcock, N. W. 1972 Calcification of cartilage. Clin. Orthop., *86:* 287–311.

Ali, S. Y., S. W. Sajdera and H. C. Anderson 1970 Isolation and characterization of calcifying matrix vesicles from epiphyseal cartilage. Proc. Nat. Acad. Sci., *67:* 1513–1520.

Anderson, H. C. 1968 Vesicles in the matrix of epiphyseal cartilage: Fine structure, and association with calcification. In: Proceedings of the 4th European Regional Conference on Electron Microscopy. Vol. 2. Rome, Tipagrafia Poliglotta Vatacana, pp. 437–438.

———— 1969 Vesicles associated with calcification in the matrix of epiphyseal cartilage. J. Cell Biol., *41:* 59–72.

Anderson, H. C., T. Matsuzawa, S. W. Sajdera and S. Y. Ali 1970 Membranous particles in calcifying cartilage matrix. Trans. N. Y. Acad. Sci., *32:* 619–628.

Anderson, H. C., and S. W. Sajdera 1971 The

fine structure of bovine nasal cartilage. Extraction as a technique to study proteoglycans and collagen in cartilage matrix. J. Cell Biol., *49:* 650–663.

Bernard, G. W. 1972 Ultrastructural observations of initial calcification in dentine and enamel. J. Ultrastruct. Res., *41:* 1–17.

Bonucci, E. 1967 Fine structure of early cartilage calcification. J. Ultrastruct. Res., *20:* 33–50.

——— 1969 Further investigation on the organic/inorganic relationships in calcifying cartilage. Calcif. Tissue Res., *3:* 38–54.

——— 1970 Fine structure and histochemistry of "calcifying globules" in epiphyseal cartilage. Z. Zellforsch., *103:* 192–217.

——— 1971 The locus of initial calcification in cartilage and bone. Clin. Orthop., *86:* 108 139.

Campo, R. D. 1970 Protein polysaccharide of cartilage and bone in health and disease. Clin. Orthop., *68:* 182–209.

Caro, L. G., and G. E. Palade 1964 Protein synthesis, storage and discharge in the pancreatic exocrine cell. An autoradiographic study. J. Cell Biol., *20:* 473–495.

Curran, R. C., A. E. Clark and D. Lovell 1965 Acid mucopolysaccharide in electron microscopy. The use of the colloidal iron method. J. Anat., *99:* 427–434.

Dearden, L. C., and H. D. Mosier 1971 Electron microscopy of tibial cartilage in catch-up growth. Anat. Rec., *169:* 304–305.

——— 1972 Long term recovery of chondrocytes in the tibial epiphyseal plate in rats after cortisone treatment: An electron microscopic study. Clin. Orthop., *87:* 322–331.

Dulce, H. J. 1960 Zur Biochemie der Verknocherung. I. Mineralgehalt und Grundsubstanzzusammensetzung des hyalinen Knorpels, des verknocherden Knorpels und des Knochens. Z. Physiol., Chemie., *319:* 257–271.

Eisenmann, D. R., and P. L. Glick 1972 Ultrastructure of initial crystal formation in dentin. J. Ultrastruct. Res., *41:* 18–28.

Foldes, I., L. Modis and I. Suveges 1965 Investigations of the mucopolysaccharides in the proximal epiphyseal cartilage of the rat: A comparison of the methods of histochemical assay. Acta Morphol. Acad. Sci. Hungary, *13:* 141–153.

Glimcher, M. J. 1960 In: Calcification in Biological Systems. Amer. Assoc. Advance. Sci., Washington, D. C., pp. 421–487.

Godman, G. C., and N. Lane 1964 On the site of sulfation in the chondrocyte. J. Cell Biol., *21:* 353–366.

Hass, G. M. 1943 Studies of cartilage. IV. A morphologic and chemical analysis of aging human costal cartilage. Arch. Path., *35:* 275–284.

Holtrop, M. E. 1972 The ultrastructure of the epiphyseal plate. I. The flattened chondrocyte. Calcif. Tissue Res., *9:* 131–139.

Jamieson, J. D., and G. E. Palade 1967 Intracellular transport of secretory proteins in the pancreatic exocrine cell. I. Role of peripheral elements of the Golgi complex. J. Cell Biol., *34:* 577–596.

Matsuzawa, T., and H. C. Anderson 1970 Phosphatases of epiphyseal cartilage studied by electron microscope histochemistry. Proc. 7th Congress Electron Microscopy, *1:* 529–530.

Matukas, V. J., B. J. Panner and J. L. Orbison 1967 Studies on ultrastructural identification and distribution of protein-polysaccharide in cartilage matrix. J. Cell Biol., *32:* 365–377.

Miller, Z. B., J. Waldman and F. C. McLean 1952 The effect of dyes on the calcification of hypertrophic rachitic cartilage in vitro. J. Exp. Med., *95:* 497–508.

Millonig, G. 1961 Advantages of phosphate buffer for $OsO_4$ solution in fixation. J. Appl. Phys., *32:* 1637.

Mowry, R. W. 1958 Improved procedure for the staining of acidic polysaccharides by Müllers colloidal (hydrous) ferric oxide and its combination with the Feulgen and the periodic acid-Schiff reactions. Lab. Invest., *7:* 566–576.

Neutra, M., and C. P. Leblond 1966 Radiographic comparison of the uptake of galactose $^3H$ and glucose $^3H$ in the Golgi region of various cells secreting glycoproteins or mucopolysaccharides. J. Cell Biol., *30:* 137–150.

Rambourg, A., W. Hernandez and C. P. Leblond 1969 Detection of complex carbohydrates in the Golgi apparatus of rat cells. J. Cell Biol., *40:* 395–414.

Reynolds, E. S. 1963 The use of lead citrate at high pH as an electron opaque stain in electron microscopy. J. Cell Biol., *17:* 208–212.

Rohr, H., and S. Walter 1966 Die Mucopolysaccharidsynthese in ihrer Beziehung zur submikroskopischen Strukter der Knorpelzelle. Acta Anat., (Basal), *64:* 223–234.

Rosenquist, T. H., B. G. Slavin and S. Bernick 1971 The Pearson silver-gelatin method for light microscopy of 0.5–2 $\mu$ plastic sections. Stain Tech., *5:* 253–257.

Schiller, S., G. A. Glover and A. Dorfman 1962 Effect of the thyroid gland on metabolism of acid mucopolysaccharides in skin. Biochem. Biophys. Acta, *58:* 27–33.

Schubert, M., and M. Pras 1968 Ground substance protein polysaccharides and precipitation of calcium phosphate. Clin. Orthop., *60:* 235–255.

Silberberg, R., M. Silberberg and D. Feir 1964 Life cycle of articular cartilage cells: An electron microscopic study of the hip joint of the mouse. Am. J. Anat., *114:* 17–48.

Silberberg, R., and M. Hasler 1966 Fine structure of articular cartilage in mice receiving cortisone acetate. Arch. Path., *82:* 569–582.

Smith, J. W. 1970 The disposition of protein polysaccharide in the epiphyseal plate cartilage of the young rabbit. J. Cell Sci., *6:* 843–864.

Sobel, A. E., J. M. Burger and S. Nobel 1960 Mechanisms of nuclei formation in mineralizing tissues. Clin. Orthop., *17:* 103–123.

Spicer, S. S. 1962 Histochemical differentiation of sulfated rodent mucins. Ann. Histochem., *7:* 23–28.

Thyberg, J., and U. Friberg 1970 Ultrastructure and acid phosphatase activity of matrix vesi-

cles and cytoplasmic dense bodies in the epiphyseal plate. J. Ultrastruct. Res., *33:* 554–573.

——— 1972 Electron microscope enzyme histochemical studies on the cellular genesis of matrix vesicles in the epiphyseal plate. J. Ultrastruct. Res., *41:* 43–59.

Thyberg, J. 1972 Ultrastructural localization of aryl sulfatase activity in epiphyseal plate. J. Ultrastruct. Res., *38:* 332–342.

Weatherell, J. A., P. J. Baily and S. M. Weidmann 1964 Sulfated mucopolysaccharides and calcification. In: Bone and Teeth. H. J. J. Blackwood, ed. Pergamon Press, Oxford, pp. 227–230.

*Abbreviations*

A, apatite
C, calcification zone
CDB, cytoplasmic dense bodies
CM, cell membrane
CV, cytoplasmic vacuole
ER, endoplasmic reticulum
G, Golgi complex
GL, glycogen
GV, Golgi vacuole
H, hypertrophic zone
L, lipid
LG, lacunar granules
M, mitochondrion
MG, matrix granules
MV, matrix vesicles
P, proliferation zone
PL, pericellular lacuna
R, reserve zone

## PLATE 1

### EXPLANATION OF FIGURES

1A,B Part of the epiphyseal plate at the end of the treatment period (1A) and in a corresponding control (1B). Paraffin, Mowry's colloidal iron (pH 1.3), PAS × 240. Comparison of these figures reveals a marked reduction of sulfated mucopolysaccharide (arrows) in the matrix of the PTU-treated rats.

2A,B Part of the epiphyseal plate at the end of the treatment period (2A) and in a corresponding control (2B). Paraffin, PAS, × 655. Intracellular glycogen deposition (white arrows) is much more prominent in the PTU-treated rats than in controls. Granules in the matrix of the PTU-treated rats (matrix vesicles, PAS-positive, black arrows) are also more prominent than they are in the matrix or controls.

3A,B Part of the hypertrophic and calcification zones showing the onset of calcification (arrows) at the end of the treatment period (3A) and in a corresponding control (3B). Epon thick sections (0.5 $\mu$), toluidine blue, × 750. Insets — hypertrophic and calcification zones to show the relative amounts of calcium deposition (arrows). Epon thick sections (0.5 $\mu$), deplasticized, Pearson silver-gelatin, × 430. Comparison of these figures and insets shows enhanced calcification and calcium deposition in the PTU-treated rats.

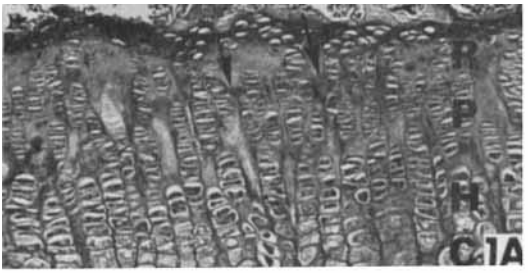
R
P
H
C
1A

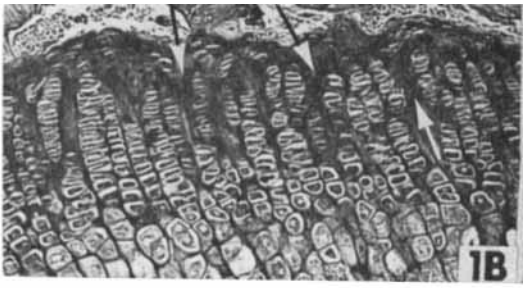
1B


2A

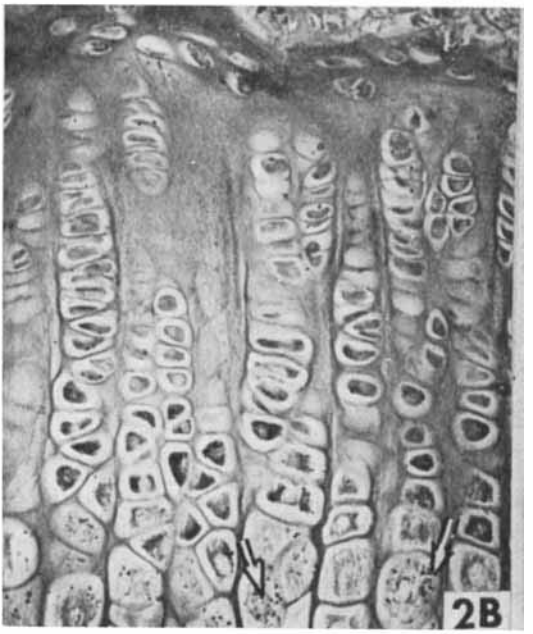
2B

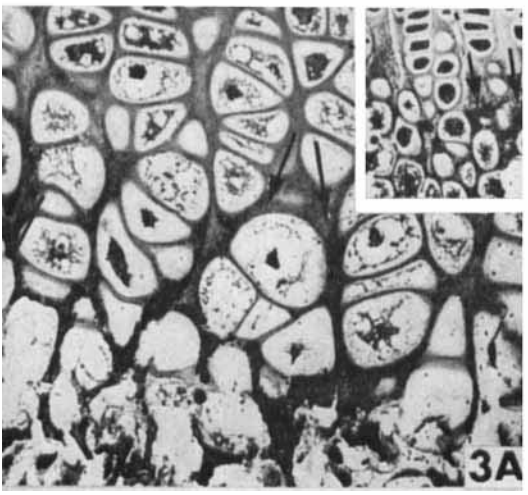
3A

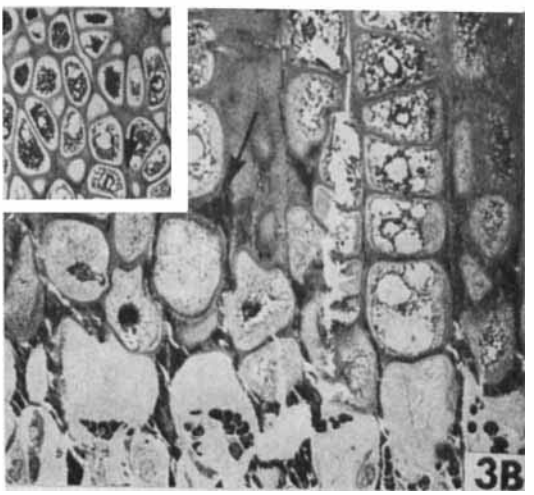
3B

## PLATE 2

### EXPLANATION OF FIGURES

4A Part of a proliferation zone chondrocyte (at the end of the treatment period) and part of its lacuna demonstrating acid mucopolysaccharide in Golgi vacuoles, in the cell membrane, at the outer aspects of cytoplasmic dense bodies, in lacunar granules, and on the outer lamina of a matrix vesicle. Glutaraldehyde fixation with post-osmication, stained with Mowry's colloidal iron. × 48,000.

4B Matrix vesicles and matrix granules in the proliferation zone at the termination of treatment showing the acid mucopolysaccharide content of matrix granules and of the surface of matrix vesicles. Collagen is negative. Glutaraldehyde fixation with post-osmication, stained with Mowry's colloidal iron. × 60,000.

4C Part of a proliferation zone chondrocyte at the termination of the treatment period, part of its lacuna, and part of the extracellular matrix. Formalin fixation with post-osmication, hyaluronidase digestion, and stained with bismuth nitrate for sulfated mucopolysaccharides. × 30,000. Note the absence of stained granules in Golgi vacuoles, on the cell membrane, in the pericellular lacuna, or in the extracellular matrix. Matrix vesicles are visible because of their osmiophilia, but no granular deposits are apparent on their outer surface.

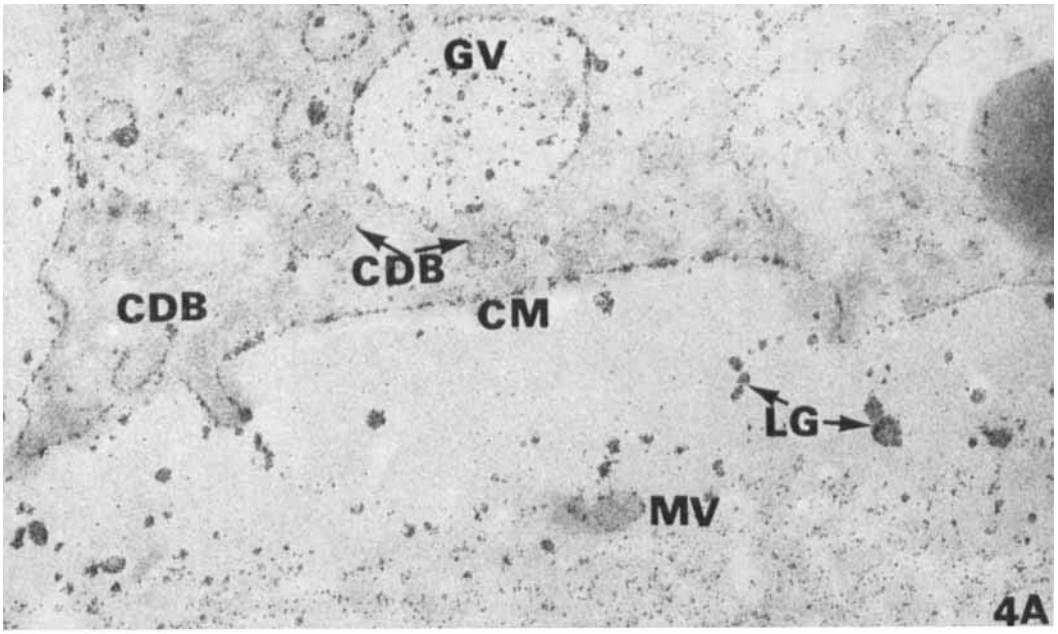
GV
CDB
CDB
CM
LG
MV
4A

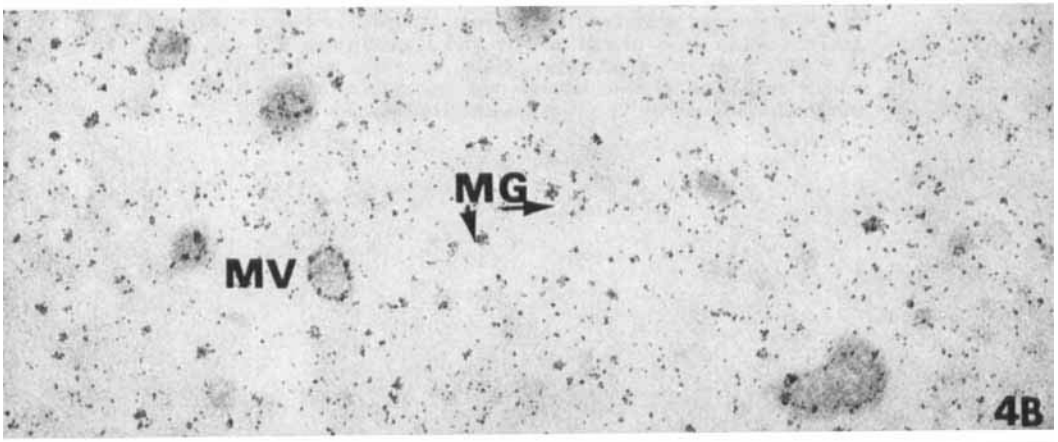
MG
MV
4B

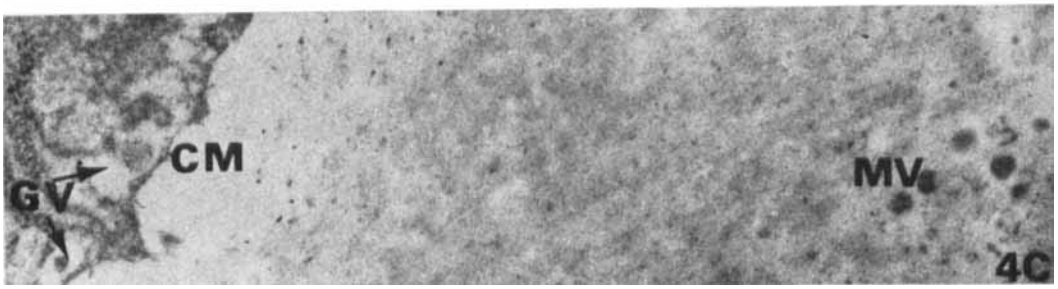
CM
GV
MV
4C

## PLATE 3

EXPLANATION OF FIGURE

5 A column of degenerate chondrocytes in the proliferation zone at the end of the treatment period. Numerous apatite crystals in the proliferation zone are depicted in the inset. This and all subsequent electron micrographs were fixed with glutaraldehyde, post-osmicated, and double stained with uranyl acetate and lead citrate. × 5,300; inset × 32,000. Note the hypertrophic Golgi vacuoles, particularly in the middle two cells. Apatite crystals are not present in the matrix in the proliferation zone in corresponding controls.

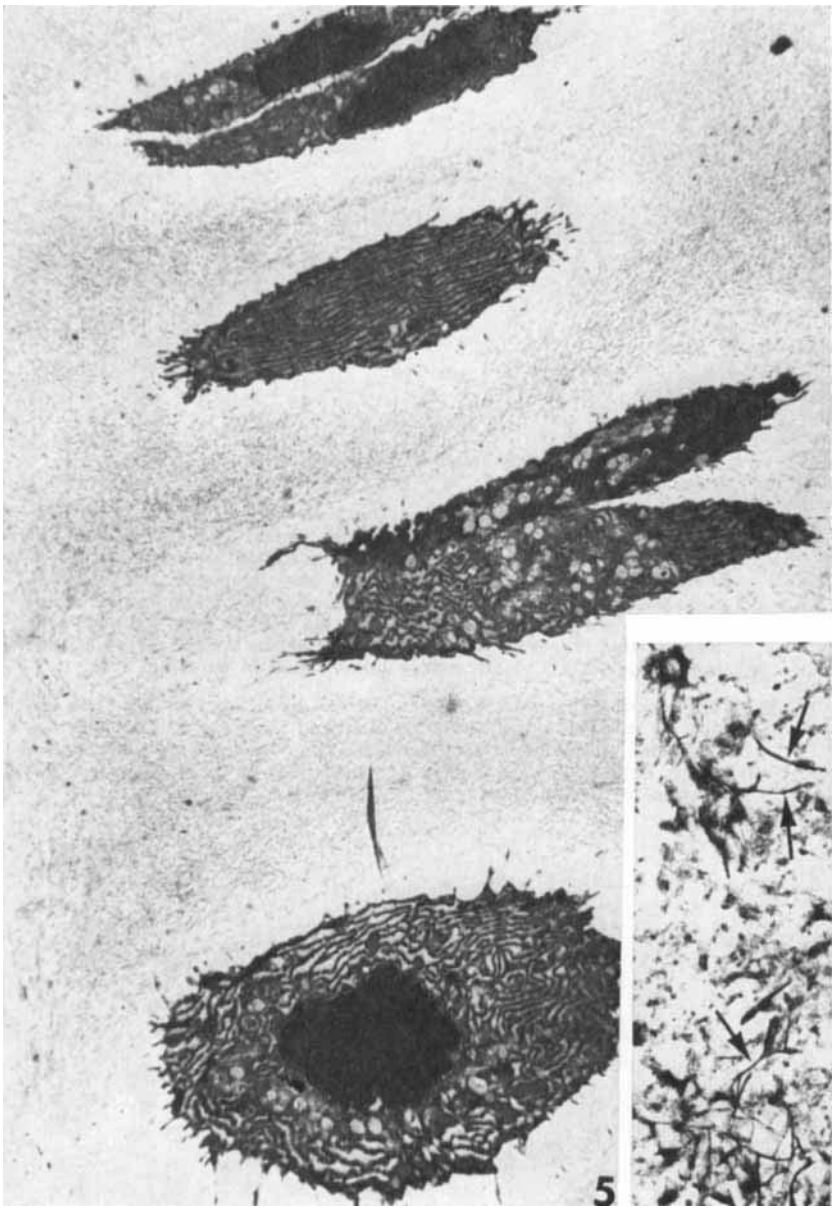
5

## PLATE 4

### EXPLANATION OF FIGURES

6A,B Reserve zone chondrocytes at the termination of the treatment period (6A) and in a corresponding control (6B). The outlined areas contain matrix vesicles and are enlarged as insets. × 4,300; insets × 60,000. When these figures are compared, considerable chondrocyte degeneration is noted in the PTU-treated rats; cytoplasmic vacuoles are common, the nucleus is not normal, and matrix vesicles, sometimes associated with apatite crystals, are more numerous and frequently larger than in controls.

6C This figure is an enlargement of a cell in figure 6A. Note the abnormal nuclear morphology, swollen and vacuolated mitochondria, enhanced cytoplasmic vacuolization, excessive and premature glycogen deposition frequently in conjunction with lipid, and a reduction in the amount of ER. × 15,000.

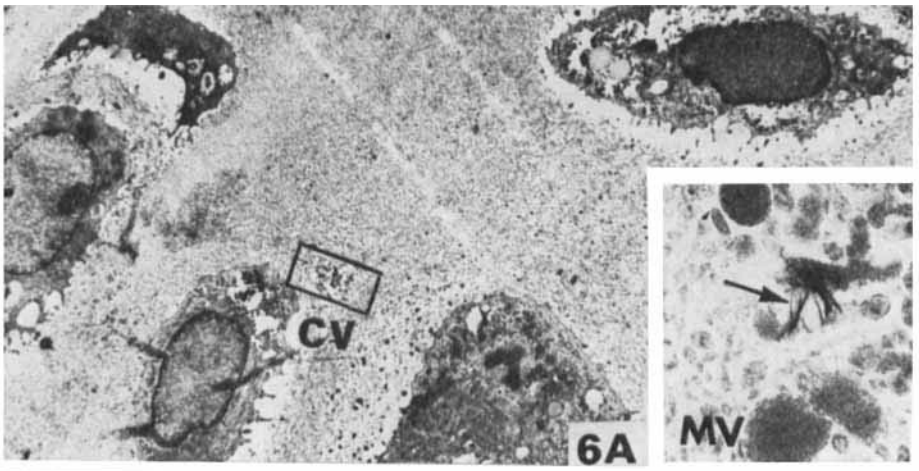
CV
6A
MV

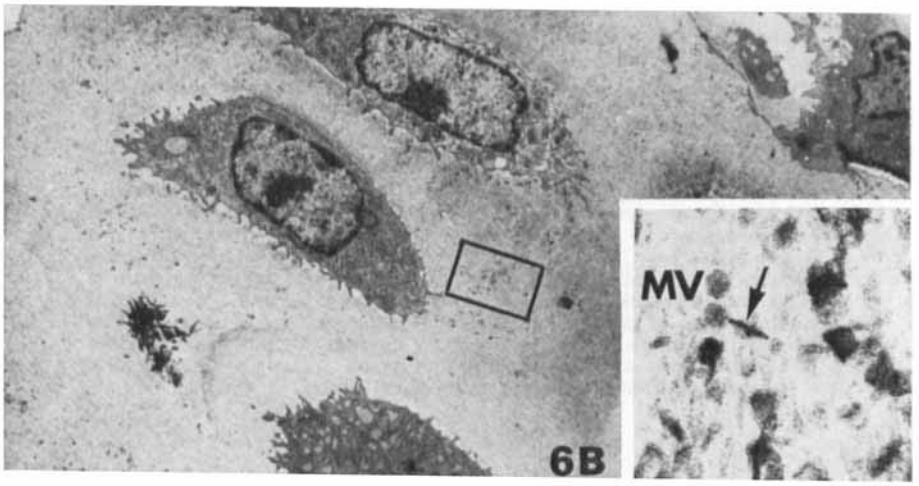
MV
6B

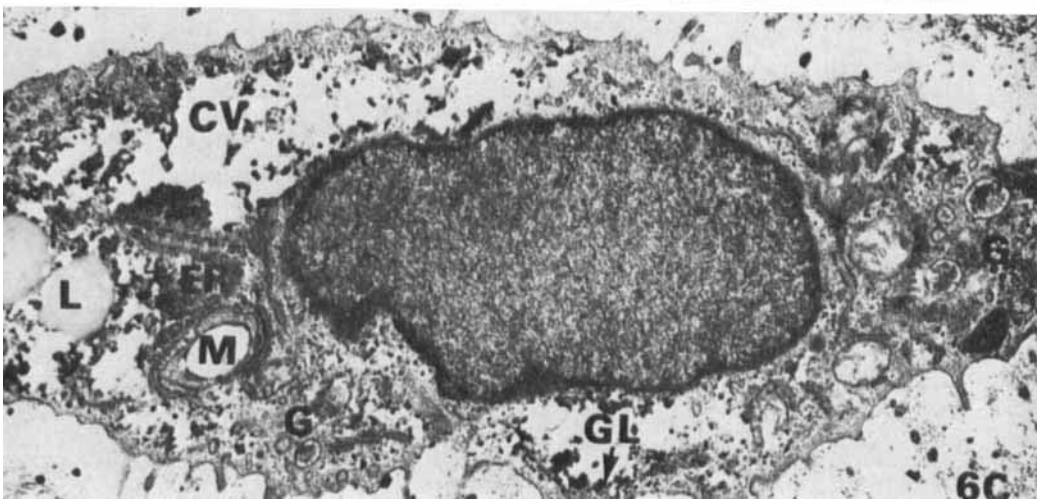
CV
L
ER
M
G
GL
6C

## PLATE 5

EXPLANATION OF FIGURES

7 Microscars (arrows), composed of dense fibrils, are numerous and indicative of cell death. The inset is an additional adjacent microscar in which banding of the collagen fibrils is distinctive. × 24,600; inset × 24,600.

8A,B These figures portray the possible genesis of matrix vesicles. In 8A, part of a "disintegrating" reserve zone chondrocyte with numerous cytoplasmic dense bodies is depicted. One cytoplasmic dense body (single arrow) along with part of the cytoplasmic ground substance seems to have entered the pericellular lacuna through a disrupted area of the cell membrane while others (double arrows) appear to be in the process of exocytosing. In 8B, from an adjacent area, the final stage of proposed chondrocyte disintegration is depicted. The cell membrane is absent, ground substance is indistinct, but the number, size, and ultrastructure of many "matrix vesicles" corresponds with that of cytoplasmic dense bodies. × 60,000.

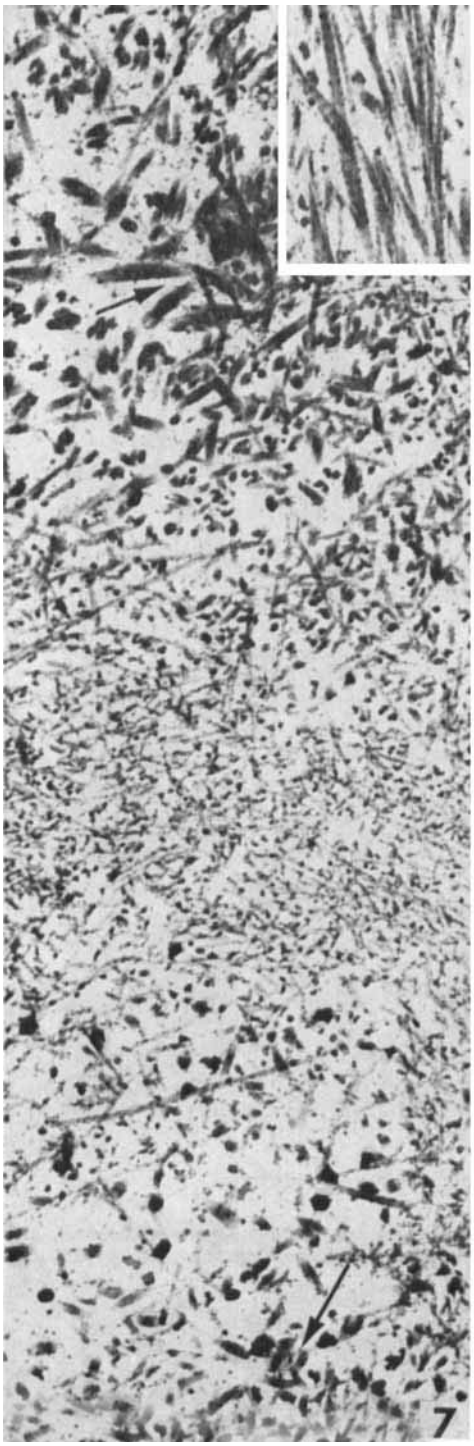
7

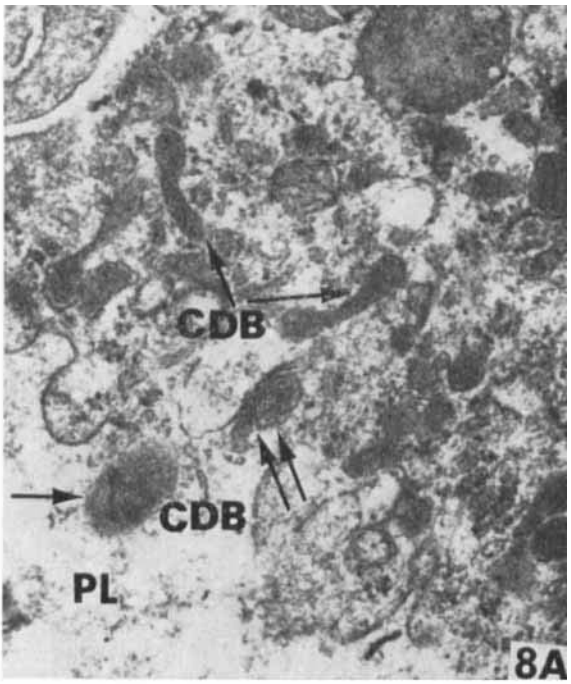
CDB
CDB
PL
8A

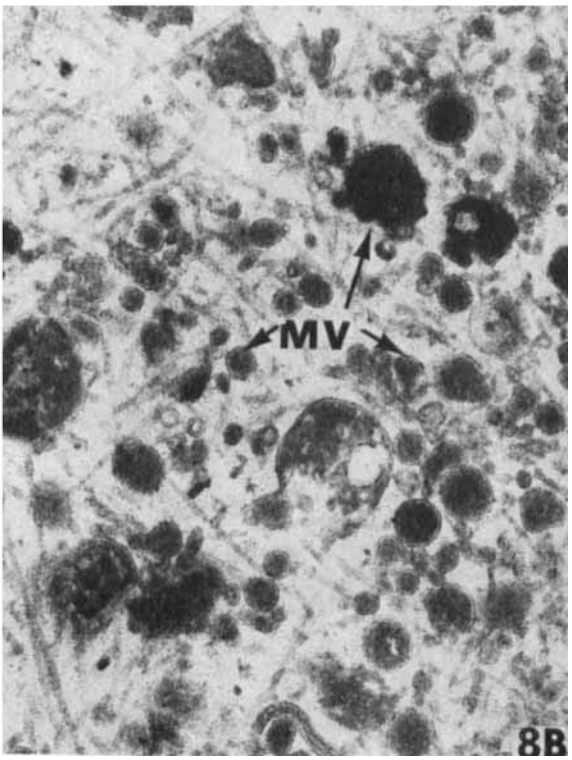
MV
8B

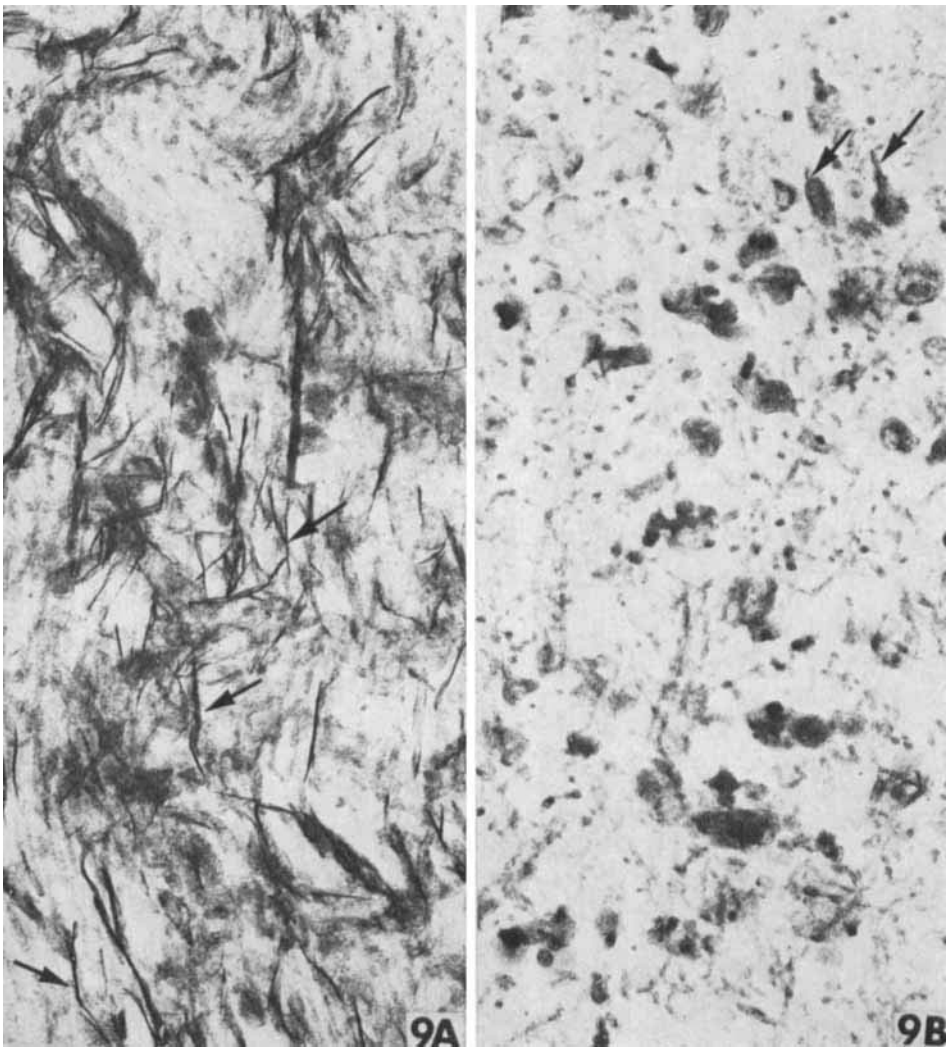


EXPLANATION OF FIGURES

9A,B Part of the extracellular matrix in the upper proliferation zone in a PTU-treated rat (9A), and from the same area in a corresponding control (9B). Note the preponderance of apatite crystals (arrows) in the PTU-treated rat. × 60,000.

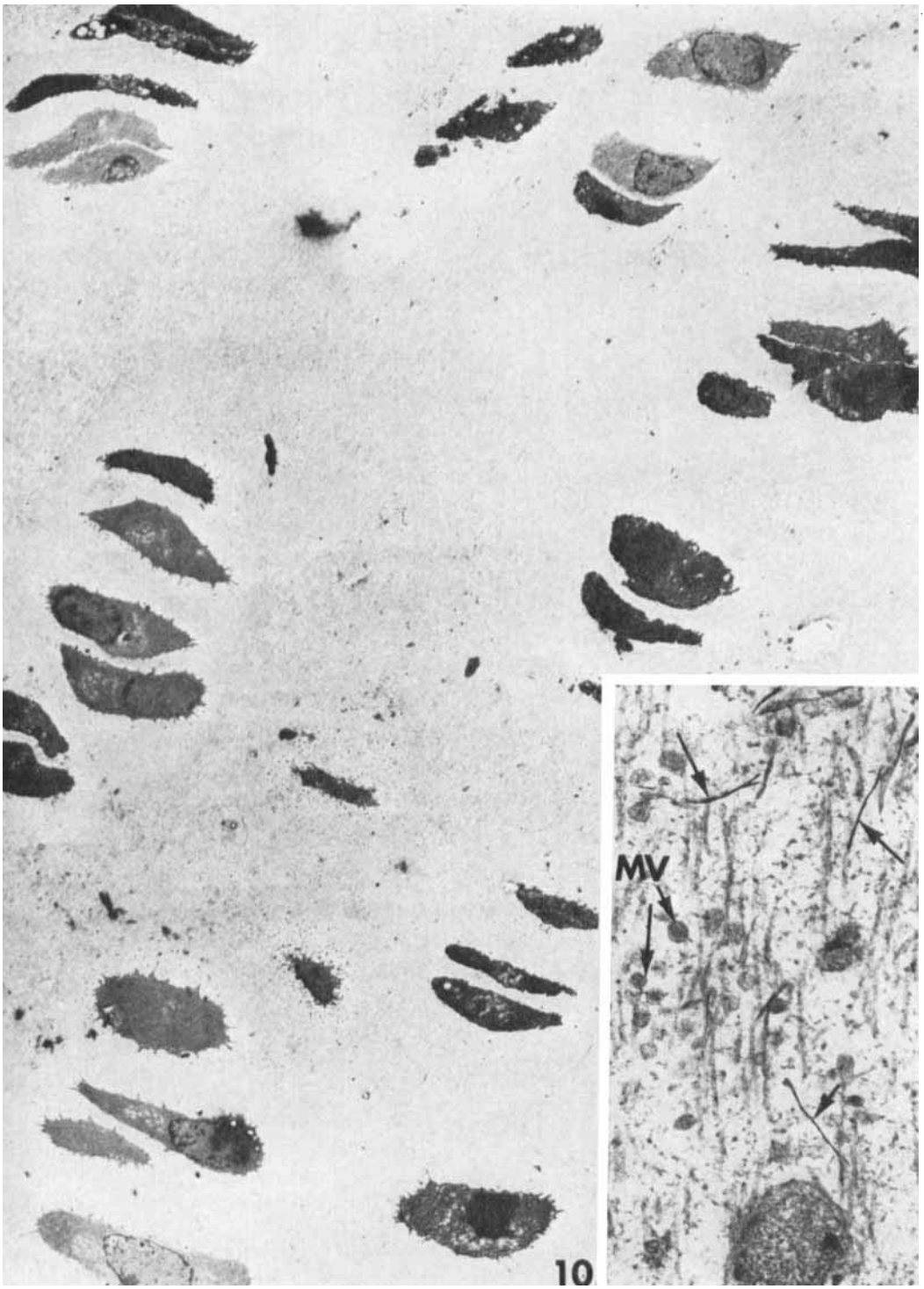


EXPLANATION OF FIGURE

10 Part of the proliferation zone in the terminal recovery period (26 days). Note the presence of a column of degenerate chondrocytes as well as scattered degenerate cells intermixed with normally appearing chondrocytes. The inset shows the persistence of apatite crystals (arrows) associated with matrix vesicles, in a longitudinal septum in the mid-proliferation zone. × 2,000; inset × 48,000.